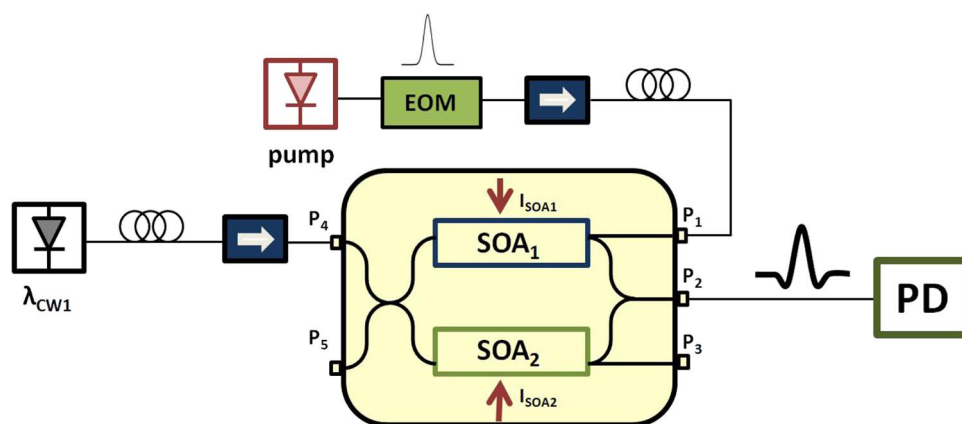


# UWB Doublet Generation Employing Cross-Phase Modulation in a Semiconductor Optical Amplifier Mach–Zehnder Interferometer

Volume 5, Number 6, December 2013

V. Moreno  
M. Rius  
J. Mora  
M. A. Muriel, Senior Member, IEEE  
J. Capmany, Fellow, IEEE



# UWB Doublet Generation Employing Cross-Phase Modulation in a Semiconductor Optical Amplifier Mach–Zehnder Interferometer

V. Moreno,<sup>2</sup> M. Rius,<sup>1</sup> J. Mora,<sup>1</sup> M. A. Muriel,<sup>2</sup> *Senior Member, IEEE*, and J. Capmany,<sup>1</sup> *Fellow, IEEE*

<sup>1</sup>ITEAM Research Institute, Universitat Politècnica de València, 46022 València, Spain

<sup>2</sup>Department of Photonics Technology and Bioengineering, ETSIT, Universidad Politécnica de Madrid (UPM), 28040 Madrid, Spain

DOI: 10.1109/JPHOT.2013.2288295  
1943-0655 © 2013 IEEE

Manuscript received September 26, 2013; revised October 23, 2013; accepted October 23, 2013. Date of publication November 4, 2013; date of current version November 11, 2013. This work was supported in part by national projects TEC2010-21303-C04-02 and TEC2011-26642 under the responsibility of the Ministerio de Economía y Competitividad, by projects FEDER UPVOV08-3E-008 and UPVOV10-3E-492, and by the Generalitat Valenciana under the Research Excellency Award Program GVA PROMETEO 2013/012 Next Generation Microwave Photonic technologies. Corresponding author: J. Mora (e-mail: jmalmer@iteam.upv.es).

**Abstract:** In this paper, a novel method to generate ultrawideband (UWB) doublets is proposed and experimentally demonstrated, which is based on exploiting the cross-phase modulation in a semiconductor optical amplifier (SOA). The key component is an integrated SOA Mach–Zehnder interferometer pumped with an optical carrier modulated by a Gaussian pulse. The transfer function of the nonlinear conversion process leads to the generation of UWB doublet pulses by tuning the SOA currents to different values.

**Index Terms:** Interferometric structure, nonlinear optics, microwave photonics, fiber optics, optical communications.

## 1. Introduction

Microwave photonics (MWP) technologies have been developed as an interdisciplinary area connecting the application fields of microwave and optics. MWP provides features and possibilities that are very difficult or even unachievable with standard RF technologies such as tunability and reconfigurability [1]. In the past few years, there has been an increasing effort in researching new MWP methods for various applications [2]. In particular, Ultra-wideband over fiber (UWBoF) has been proposed [3], [4] as a result of the low power density of the transmitted signal.

Ultra-wideband (UWB) has emerged as an attractive solution for novel high data rate and short range wireless communication systems. The U.S. Federal Communications Commission (FCC) defines UWB as any signal that occupies more than 500 MHz bandwidth or possesses a fractional bandwidth greater than 20%. In this context, the FCC has also approved the unlicensed use of a spectral band from 3.1 to 10.6 GHz with a transmitted power spectral density (PSD) less than  $-41.3$  dBm/MHz for indoor wireless communications. The interest in this technology is due to its advantages in terms of low power usage, high data rates, precise positioning capabilities, extremely low interference and particularly the ability to spread a signal over a wide bandwidth, ensuring a low power density and thus being capable of coexisting with other wireless technologies [5]. The

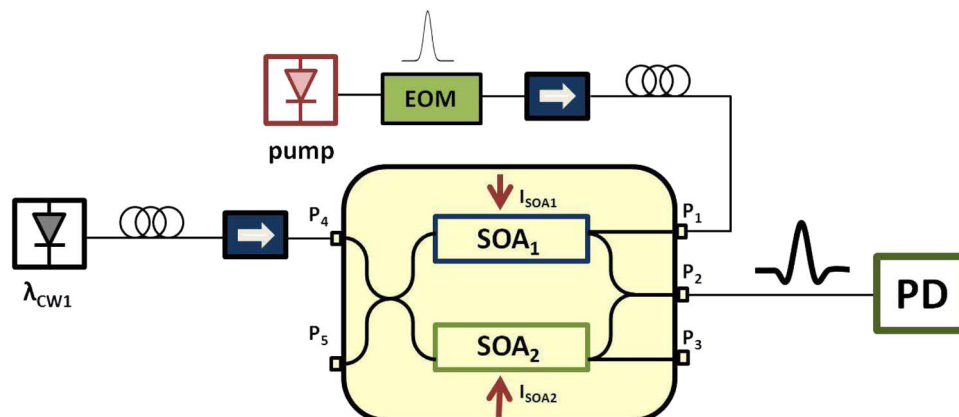


Fig. 1. Experimental setup based on a SOA-MZI.

range of distance of an UWB scheme is limited from a few meters to tens of meters and UWBoF permits to extend the area of coverage distribution over fiber. At this point, the combination of MWP and UWB technologies has demonstrated to be widely interesting. However, distribution is not the only advantage brought by MWP, major applications of MWP systems include photonic generation, processing, control and distribution of microwave signals [2], [6].

In this context, the generation of UWB pulses has benefited from the proposal of several methods involving the use of optical techniques [7]–[10]. Furthermore, the use of SOAs, in particular, provides several advantages in all-optical generation by exploiting their nonlinear effects, low power consumption, flexibility and scalability. These implementations can be classified according to the non-linearity taken into consideration as four-wave-mixing (FWM) [11], cross-gain modulation (XGM) [12] and cross-phase modulation (XPM) [13].

In this paper, we propose and experimentally demonstrate a novel scheme to generate UWB doublets based on exploiting the nonlinearities present in an integrated interferometric structure. The key component of the system is the SOA-MZI composed of two SOAs. The conversion process depends directly of the currents applied in each branch. A pump signal is introduced to the setup to induce the XPM effect in the SOA-MZI and as a result of the non-linear characteristics of the transfer function we can achieve the generation of UWB doublets at a specific operation point that is dictated by the saturation of the SOAs. Our approach yields the desired waveform and represents a simpler solution compared to previous configurations. In addition, the interferometric structure permits to potentially scale the scheme to generate higher order pulses necessary for UWB communication systems with more stringent requirements

The rest of the paper is organized as follows. In Section 2, we analyze the operation principle of the proposed scheme. Through the transfer function of the system, we present the parameters that allow the control of the SOA-MZI conversion process. The ability to control the UWB pulse polarity by means of the applied bias current is also verified. In Section 3, we present the experimental results showing the system performance with the UWB doublets and we compare our results with previous reports. Finally, conclusions are presented in Section 4.

## 2. Principle of Operation

Fig. 1 shows the experimental configuration of the proposed scheme to generate UWB doublets by means of an integrated SOA-MZI containing two 1-mm InGaAsP-InP SOAs with low polarization sensitivity. The system is composed of a continuous wave signal source (labeled as  $\lambda_{CW1}$ ), the mentioned interferometric structure, a pump source providing the input time-varying signal and a photodetector. In principle, cross-gain modulation (XGM) and cross-phase modulation (XPM) processes can be present in the SOAs. However, the linewidth enhancement factor of the SOAs is large enough to neglect the XGM effect.

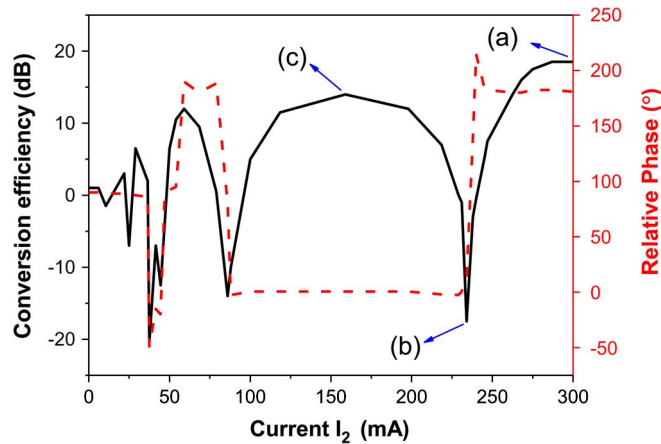


Fig. 2. Transfer function of the SOA-MZI: Conversion amplitude at the output port  $P_2$  (solid black line) and the corresponding relative phase between input port  $P_1$  and output port  $P_2$  (red dashed line). Representative operation points are labeled with letters a, b and c. Maximum conversion with a quasi-linear response corresponds with points (a) and (c) whereas minimum conversion with a quadratic response corresponds with point (b).

The main component of this architecture is the SOA-MZI, described in detail in [14] and operated in counter-propagation configuration. For this experimental setup, the employed pump signal is obtained by external electro-optical modulation of a continuous wave (CW) optical carrier with an optical wavelength ( $\lambda_{pump}$ ) centered at 1535.04 nm. As appreciated in Fig. 1, the pump signal is launched into the system through port  $P_1$  and the CW laser source into port  $P_4$  (the corresponding wavelength of  $CW_1$  is 1550.12 nm). Since the conversion process is carried out in counter-propagation configuration, optical filtering is not needed to separate the pump from the probe signal. Finally, the signal obtained through the XPM process is measured at port  $P_2$  by means of a photodetector (PD) and it is also analyzed in an oscilloscope or a spectrum analyzer.

The XPM process in the SOA-MZI depends on the average optical power of the pump and probe signals, and at the same time on the electrical currents applied to each SOA [14]. Consequently, the optical power of both (pump and probe) signals must be controlled in order to optimize the conversion process. For this implementation, the values for the optical power of the pump and probe signals were established at 13.0 dBm and 5.4 dBm, respectively.

Fig. 2 plots the conversion transfer function of the proposed configuration. It is possible to identify the different conversion points and the advantages and limitations of each one of these by analyzing the transfer function. The experimental characterization was obtained by modulating the pump signal with an RF tone at a frequency of 10 GHz generated and analyzed by a lightwave component analyzer (LCA). Fig. 2 plots the conversion efficiency factor and the relative phase between the output signal at the port  $P_2$  and the pump signal launched into port  $P_1$  as a function of the electrical current applied to SOA2 ( $I_2$ ). We kept the value for the current applied to SOA1 ( $I_1$ ) fixed to 300 mA, which value defines the speed conversion of the probe continuous signal. In the proposed scheme, different operation stages can be achieved to perform a conventional conversion. For the applied currents ( $I_1$  and  $I_2$ ), the maximum XPM conversion point is found to be achieved when a current of 300 mA is applied to SOA2.

The transfer function is measured by means of a RF tone in low modulation regime. As shown in Fig. 2, the operation point (a) corresponds with a maximum conversion with a quasi-linear response between the output and input RF modulation. The operation point (b) features a conversion minimum to a SOA-MZI transfer function with a quadratic response. In this context, the nonlinear response of the transfer function can be achieved for currents far from maximum operation points, following a similar approach to proposals based on the transfer function of an EOM [15]. In our case, the conversion efficiency reveals noticeable improvements. Moreover, additional maximum operation points as (c) are achieved for lower currents. Also, we can observe in Fig. 2 how the

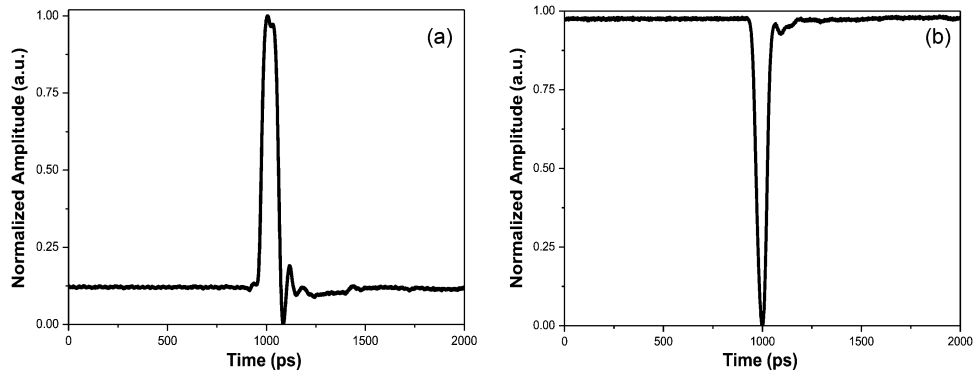


Fig. 3. (a) Electrical pulsed signal and (b) optical signal at the output of EOM which represents the pump signal.

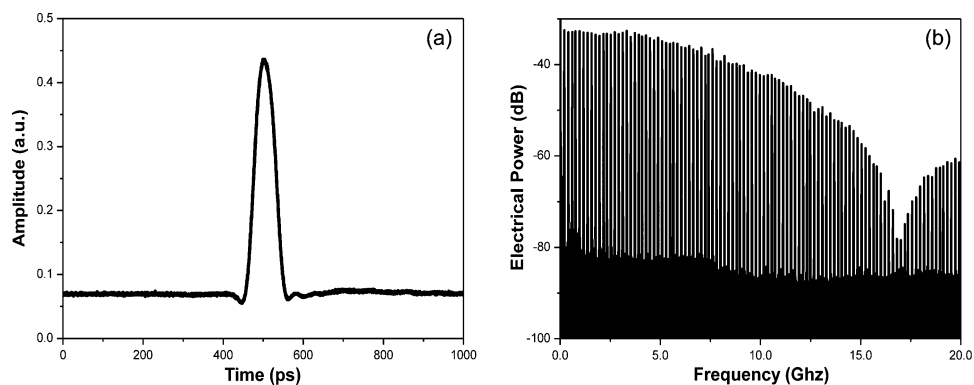


Fig. 4. (a) Waveform and (b) spectrum obtained at port  $P_2$  with  $I_2 = 300$  mA.

relative phase between the output and input signal changes from  $0^\circ$  to  $180^\circ$  for different regions and concretely for operation points (a) and (c). This change of sign leads to a control of the UWB pulse polarity as a function of the applied bias current.

### 3. Experimental Results

In order to demonstrate the UWB generation approach, an experiment has been carried out according to Fig. 1. The pump laser was externally modulated with a quasi-Gaussian pulse train. The electrical signal that is introduced into the EOM has a fixed pattern of one “1” and sixty-three “0”, summing up a total of 64 bits with a bit rate of 12.5 Gb/s. Fig. 3(a) shows the equivalent pulse to the input of the EOM and Fig. 3(b) plots the optical output of the EOM corresponding to the time varying optical pump signal. It is important to mention that the EOM is biased in a negative region so an inverted pulse is obtained which is essential to guarantee the saturation of the SOA1 with high level of power coming from the pump signal.

As it was shown in Fig. 1, the pump signal is introduced into Port 1 ( $P_1$ ), the probe signal into the port  $P_4$  and the system output is obtained at port  $P_2$  where a PD is connected to detect the RF signal. As previously mentioned, it was important to control the operation currents for SOA1 and SOA2. In this case, the operation current for SOA1 ( $I_1$ ) is set at 300 mA, but the value for  $I_2$  is gradually modified in order to measure the resulting waveform and spectrum through a digital communication analyzer (DCA) and an electrical spectrum analyzer (ESA). First, a current of 300 mA is applied to SOA2. Such current value corresponds to an operation region in the transfer function with negative slope. As expected, the output pulse is inverted leading to the generation of a quasi-Gaussian pulse as shown in Fig. 4(a). The corresponding spectrum is visualized in Fig. 4(b).

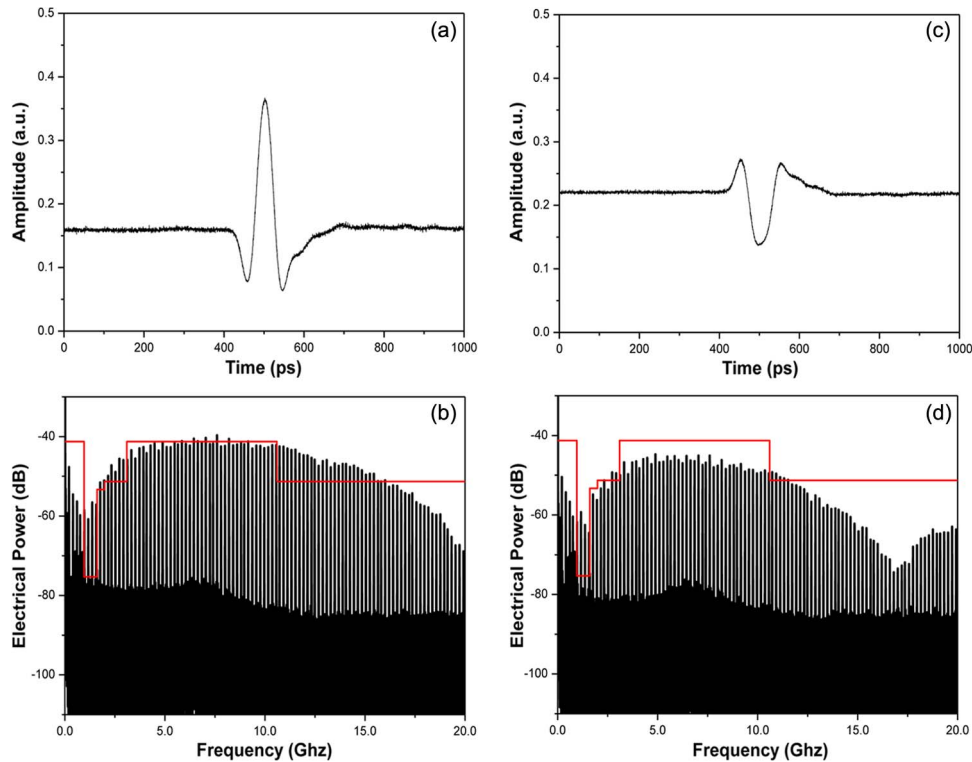


Fig. 5. (a) Waveform and (b) electrical spectrum of the UWB doublet pulse for an electrical current applied to SOA2 of 270 mA. (c) Waveform and (d) electrical spectrum of the UWB doublet pulse for an electrical current applied to SOA2 of 176 mA.

If the current is continuously tuned, it is possible to observe different waveforms through the complete working cycle of the SOA-MZI. Once we perform such process, we select the two stages that best fit the conditions for generating a doublet. When the electrical current of SOA2 is tuned to 270 mA, the input pulse is large enough to saturate the interferometric structure (SOA-MZI) and therefore a doublet pulse is generated. In this context, it is also feasible to switch the polarity of the obtained doublet pulse by modifying the value of  $I_2$  and setting it at 176 mA. Fig. 5(a) and (b) plot the waveform and corresponding spectrum for the measurement performed at  $I_2 = 270$  mA. Fig. 5(c) and (d) reveal these same parameters but with a current value of 176 mA. By comparing the characteristics of the obtained doublet pulses, we can determine that the amplitude of the UWB doublet in Fig. 5(a) is much higher than the one shown in Fig. 5(c). The reason is due to the fact that the conversion efficiency is lower for a current of 176 mA than for 270 mA as shown in Fig. 2. In addition, Fig. 5 includes the FCC mask in the electrical spectrum of each doublet pulses. When the obtained spectrum is analyzed in terms of the FCC mask, we observe that RF power could be reduced at levels where FCC requirements are accomplished. For practical applications in order to solve limitations in terms of maximum emission by means of a UWB antenna, an additional filtering stage could be considered.

Comparing with previous works using SOAs [11]–[13], we obtain a better performance in terms of noise characteristics as the MZI structure improves the extinction ratio of the conversion process [15]. Recently, a photonic approach based on an optical carrier phase-shifting method by cascading PoIMs has been presented [7]. The generated pulse complies with the FCC mask but reconfiguration or scalability is more complex compared to our proposal as it involves the manipulation of polarization states. Other reported techniques which are based on PM to IM conversion [8] and birefringence tailored time delays using SOAs [9] suffer from scalability problems. Alternate schemes for the generation of higher order derivatives exist leading to a better power efficiency [10], but at the expense of considerable system complexity. In contrast, our approach permits to obtain a

high performance having the potential to easily achieve higher order pulses by increasing the number of optical carriers. In principle, the use of EOMs and SOAs could increase the complexity in the experimental assembly. However, the last advances on photonic integrated circuits (PIC) lead to the introduction of EOMs, SOAs and even AWGs on a single chip showing enhanced features and robustness as well as reduction of size, weight, cost and power consumption [16]. Very recently an IR-UWB pulse shaping through a PIC frequency discriminator has been demonstrated [17]. Therefore, progress and availability of PIC technologies increase the viability of the propose scheme for future improvements.

#### 4. Conclusion

A new procedure to generate UWB doublet pulses based on the XPM effect present in a SOA-MZI has been proposed and experimentally demonstrated. A modulated optical pulse is employed as a pump signal to convert the input optical signal into a doublet through an integrated SOA-MZI. The experimental analysis of the transfer function permits to identify the optimum operation point, which leads to the capacity of generating the desired doublet by means of the electrical currents applied to each SOA that compose the interferometric structure. For this application, the waveform of UWB pulses is controlled by tuning different values for the current applied to SOA2 and keeping fixed that applied to SOA1. Once the relation between the non-linear response and the current value is found, it is also possible to control the polarity of the obtained pulse by switching the value of the current applied to SOA2.

---

#### References

- [1] J. Capmany and D. Novak, "Microwave photonics combines two worlds," *Nat. Photon.*, vol. 1, no. 6, pp. 319–330, Jun. 2007.
- [2] J. Yao, "Microwave photonics," *J. Lightwave Technol.*, vol. 27, no. 3, pp. 314–335, Feb. 2009.
- [3] S. Pan and J. Yao, "Performance evaluation of UWB signal transmission over optical fiber," *IEEE J. Sel. Areas Commun.*, vol. 28, no. 6, pp. 889–900, Aug. 2010.
- [4] C. Tan, L. Ong, M. Lee, B. Luo, and P. Tang, "Direct transmission of ultra wide band signals using single mode radio-over-fiber system," *Proc. APMC*, vol. 2, pp. 1–3, Dec. 2005.
- [5] W. Su, "Ultrawideband signals and systems in communication engineering, [Book Review]," *IEEE Signal Process. Mag.*, vol. 25, no. 5, pp. 122–123, Sep. 2008.
- [6] J. Capmany, J. Mora, I. Gasulla, J. Sancho, J. Lloret, and S. Sales, "Microwave photonic signal processing," *J. Lightwave Technol.*, vol. 31, no. 4, pp. 571–586, Feb. 2013.
- [7] W. Li, L. Wang, J. Zheng, M. Li, and N. Zhu, "Photonic generation of UWB signals with large carrier frequency tunability based on an optical carrier phase-shifting method," *IEEE Photon. J.*, vol. 5, no. 5, p. 5502007, Oct. 2013.
- [8] F. Zeng, Q. Wang, and J. Yao, "All-optical UWB impulse generation based on cross-phase modulation and frequency discrimination," *Electron. Lett.*, vol. 43, no. 2, pp. 121–122, Jan. 2007.
- [9] H. Chen, M. Chen, and J. Zhang, "UWB monocycle and doublet pulses generation in optical domain," in *Proc. IEEE Topical Meet. MWP*, Oct. 2007, pp. 145–148.
- [10] M. Bolea, J. Mora, B. Ortega, and J. Capmany, "Optical UWB pulse generator using an N tap microwave photonic filter and phase inversion adaptable to different pulse modulation formats," *Opt. Exp.*, vol. 17, no. 7, pp. 5023–5032, Mar. 2009.
- [11] J. Dong, X. Zhang, Y. Zhang, and D. Huang, "Optical UWB doublet pulse generation using multiple nonlinearities of a single SOA," *Electron. Lett.*, vol. 44, no. 18, pp. 1083–1085, Aug. 2008.
- [12] M. Ran, B. Lembrikov, and Y. Ben Ezra, "Ultra-wideband radio-over-fiber concepts, technologies and applications," *IEEE Photon. J.*, vol. 2, no. 1, pp. 36–48, Feb. 2010.
- [13] F. Wang, J. Dong, E. Xu, and X. Zhang, "All-optical UWB generation and modulation using SOA-XPM effect and DWDM-based multi-channel frequency discrimination," *Opt. Exp.*, vol. 18, no. 24, pp. 24 588–24 594, Nov. 2010.
- [14] M. Manzanedo, J. Mora, and J. Capmany, "Continuously tunable microwave photonic filter with negative coefficients using cross phase modulation in a SOA-MZ interferometer," *IEEE Photon. Technol. Lett.*, vol. 20, no. 7, pp. 526–528, Apr. 2008.
- [15] Q. Wang and J. Yao, "UWB doublet generation using nonlinearly biased electro-optic intensity modulator," *Electron. Lett.*, vol. 42, no. 22, pp. 1304–1305, Oct. 2006.
- [16] L. Coldren, "Photonic integrated circuits for microwave photonics," in *Proc. IEEE Topical Meet. MWP*, Oct. 2010, pp. 1–4.
- [17] D. Marpaung and C. Roeloffzen, "Integrated microwave photonics for phase modulated systems," in *Proc. IEEE IPC*, Sep. 2012, pp. 84–85.